Reduced endothelial activation upon human blood perfusion of pig kidney xenografts lacking MHC class I and three xenoantigens

Lin Lin
Department of Biomedicine, Aarhus University https://orcid.org/0000-0002-7546-4948
Franca Witjas
LUMC
Konrad Fischer
Technische Universität München
Marten Engelse
LUMC
Annemarie de Graaf
LUMC
Beate Rieblinger
Technische Universität München
Andrea Fischer
Technische Universität München
Ying Wang
Technische Universität München
Monica Herrera
Technische Universität München
Anastasia Milusev
Department of Biomedical Research (DMBR), University of Bern, Bern
Fei Wang
Department of Biomedicine, Aarhus University
Xue Liang
BGI-Qingdao
Xi Xiang
Aarhus University
Lin Xie
MGI, BGI-Shenzhen
Ping Liu
MGI, BGI-Shenzhen
Fang Chen

MGI, BGI-Shenzhen, Shenzhen

Hui Jiang

MGI, BGI-Shenzhen

Huanming Yang

BGI-Shenzhen

Lars Bolund

Danish Regenerative Engineering Alliance for Medicine (DREAM), Department of Biomedicine, Aarhus University

Alain Despont

Department for Biomedical Research (DBMR), University of Bern, Bern

Robert Rieben

https://orcid.org/0000-0003-4179-8891

Katja Steiger

Institute of Pathology, School of Medicine, Technical University of Munich; https://orcid.org/0000-0002-7269-5433

Cees van Kooten

Leiden University Medical Center

Angelika Schnieke

TU Munich

Ton Rabelink

Leiden University Medical Centre

Yonglun Luo (alun@biomed.au.dk)

Aarhus University https://orcid.org/0000-0002-0007-7759

Article

Keywords: Xenotransplantation, Regenerative Medicine, Single Cell RNA sequencing, Kidney transplantation, Endothelial Cells

Posted Date: January 5th, 2022

DOI: https://doi.org/10.21203/rs.3.rs-1146675/v1

Abstract

Genetically tailored pigs to eliminate human immune rejection of xenografts is one promising solution to the global donor organ shortage. The development of xenograft transplantation has however been hampered by incomplete understanding of its immune rejection and the inability to test this in a human transplantation setting. Here we use an ex vivo organ perfusion system with human whole blood to assess the initial immune activation within the xenograft endothelium at single cell transcriptome level. Renal injury, complement deposition, coagulation and lymphocyte influx are all strongly reduced in genetically modified pig kidneys with porcine MHC class I and three xenoantigens (GGTA1, CMAH, B4GALNT2) eliminated (4KO) compared to wildtype (WT) pig kidneys after 6-hours human blood perfusion. Single cell RNA sequencing of endothelial cells (EC) from 4KO and WT pig kidneys respectively reveal that there is a compartment (cortex, glomeruli and medulla) specific endothelial activation, with cortical and glomeruli endothelial cells being more affected. Differential gene expression analysis shows a downregulation of endothelial transcriptome activation response to human blood perfusion in the 4KO ECs. Pathway enrichment analysis further identify the NF-kB pathway as strongly activated in human blood perfused WT ECs but diminished in the 4KO. In conclusion, the 4KO pig model has strongly reduced endothelial immune activation response when perfused with human whole blood, that goes beyond prevention of humoral rejection. Our data support further development of the 4KO for use in clinical transplantation.

Introduction

Kidney transplantation is currently the best available therapy for patients with end stage renal diseases, however organ shortage limits this treatment option [1]. Xenotransplantation with organs from genetically modified animals would provide the possibility to resolve the donor shortage problem. Pigs are considered the most suitable animal candidate given their similarity in organ size and physiology to humans, and attempts to use pig kidneys in xenotransplantation have started since the 1960s [2]. However, genetic discrepancies cause major barriers, such as the risk of viral transmission and particularly xenograft immune rejection, hampering the realization of this strategy.

A number of genetically tailored pigs have been generated to reduce the risk of viral transmission and alleviate xenograft immune rejections over the last two decades [3–10]. Initial approaches were to prevent complement activation and coagulation by overexpressing e.g. human decay-accelerating factor (hCD55) and human membrane cofactor protein (hCD46) in pigs, which significantly increase kidney graft survival in recipient non-human primates (NHP). However, acute and delayed antibody-mediated xenograft rejection still lead to graft failure. The identification of the major pig xenoantigen (α-1,3-Gal) and the subsequent generation of Gal knockout pigs was the first step towards the prevention of acute vascular rejection caused by preformed antibodies of the recipient binding to carbohydrate structures on porcine endothelial cells [4]. Afterwards, additional xenoantigens were identified including the swine leukocyte antigen complex I (SLA-I), N-glycolylneuraminic acid (Neu5Gc), β1,4 N-acetylgalactosaminyl-transferase

(B4GALNT2) [11, 12]. Recently, major breakthroughs in xenotransplantation have been further made largely due to introduction of CRISPR gene editing (CRISPR-Cas) in pigs. Complete inactivation of the porcine endogenous retroviruses (PERV) in pigs was achieved by CRISPR editing [5, 6]. With a strategy of multiplex CRISPR gene editing and transposon mediated transgenesis, genetically modified pigs with three xenoantigens removed and overexpression of nine human xenoprotective transgenes have been generated [13]. Currently, the longest reported functional graft survival (435 days) of kidney transplants in rhesus monkey is from a TKO (GTKO/β4GalKO/CMAHKO) pig with administration of anti-CD154 mAb–based regimen [14].

However, despite these great achievements made in clinical pig kidney xenotransplantation, a good system for evaluation and better understanding of the precise cellular and molecular reactions in a more ethics-friendly and human-like system is still lacking. Ex vivo machine perfusion models have been developed to extend preservation time of donor organs, perform organ quality assessment and improve organ function before transplantation [15, 16]. For example, Langin et al. demonstrated that cold perfusion with a blood based oxygenated solution prior to transplantation improved cardiac function after a pig-to-baboon heart transplant [10, 17]. Here, we use a custom-made organ perfusion system with whole blood to mimic the acute rejection response that would occur upon xenograft transplantation.

Endothelial cells (ECs) play a key role in initiating xenograft immune rejection, both with respect to the acute humoral response as well as the cellular infiltration of the xenograft. Under physiological conditions, the endothelium is actively maintaining an anti-inflammatory and anti-coagulation environment. It is therefore not surprising that almost all current genetic engineering approaches are centered on protecting the porcine endothelium. Recently, single cell transcriptional profiling of renal endothelial cells (REC) demonstrated a phenotypic heterogeneity of the renal vasculature [18]. Diverse REC populations reside within the kidney glomeruli, cortex and medulla and they are expected to play different roles during graft rejection processes. Given the highly important role of endothelial cells in xenotransplantation and the heterogeneity of (pig) endothelial cells, we investigated the initial endothelial activation response to human whole blood perfusion by single cell RNA sequencing. Our results reveal at the single cell level that human blood perfusion triggers a global transcriptome alteration in the WT pig endothelium, including the activation of endothelial inflammation and coagulation. Most importantly, our model and single endothelial cell transcriptomic analysis validate that genetic elimination of the porcine MHC class I (SLA-I) and three xenoantigens (GGTA1, CMAH, B4GALNT2) strongly reduced signs of rejection at both histology and gene expression levels in human blood perfused pig kidneys.

Materials And Methods

Ethics (for both pig and human)

Human citrated blood was obtained from the Dutch blood donor bank (Sanquin Leiden) with informed consent and ethical approval. Generation of the 4KO pigs as an experimental model for

xenotransplantation was approved by the Government of Upper Bavaria (permit number 55.2-1-54-2532-6-13) and performed according to the German Animal Welfare Act and European Union Normative for Care and Use of Experimental Animals.

Processing of blood prior perfusion

To avoid blood type incompatibility, all kidney donors (WT and KO) and blood donor (pig and human) were of blood type A. Pig blood was obtained directly during ensanguining of the pigs after which sodium citrate (11mM) was added as anticoagulant. Human citrated blood was obtained through Sanquin (www.sanquin.nl).

Processing of pig kidney prior perfusion

Pigs were slaughtered by a standardized procedure of sedative electric shock followed by exsanguination. Kidneys endured no appreciable warm ischemia time and were back-table flushed with 100 mL of cold Ringers lactate containing 12.500 I.E./ liter heparin (LEO Pharma A/S), 10mg/L butylscopolaminebromide and 1mg/L nitroglycerine. Directly after, the kidneys were flushed with 100 ml histidine-tryptophan-keteoglutarate (HTK) preservation solution containing heparin, butylscopolaminebromide and nitroglycerine and were transported on ice resulting in a cold ischemia time of maximum 2 hours.

Perfusion

The perfusion system was built around a sterilized plastic organ box, sterilized silicon perfusion tubes (LS16) (Masterflex Metrohm), a pressure probe (Edwards Lifesciences) and a custom-made pressure controller. Pressure driven perfusion at 75 mmHg MAP was achieved with a Masterflex roller pump. Sampling ports were connected through a 3-way tap (Discofix, Braun, Oss, the Netherlands). Venous and ureter flow returned to the kidney reservoir box enabling a closed perfusion loop. A clinical blood gas monitor (CDI 500 Terumo) was attached to arterial- and venous in- and outlet enabling continuous blood gas monitoring. The gas exchange was achieved through a Hillite Pediatric Oxygenator supplied with 95%O2/5% CO2. The oxygenator was connected to a circulating water bath set at 37 ˚C for heat exchange. At arrival in the laboratory the renal artery was cannulated and attached to the perfusion loop. Citrated blood (human and pig, approx. 500 mL of blood per system) was added to the systems. At T=0, T=30, T=90, T=180 and T=360 minutes perfusate samples were taken from system. Of these samples, electrolytes (sodium, potassium, chloride, calcium, glucose and urea) and gas analysis (pH, pO2, pCO2, HCO3- and lactate) were directly performed with iStat (Abbott). PH and glucose levels were adjusted accordingly during perfusion if needed.

H&E staining and histology evaluation

Cortical and medullar biopsy tissue samples were taken after 6 hours of perfusion. Tissue samples were either directly frozen using liquid nitrogen and cryopreserved at -80˚C or fixed in 4% formalin. 4-µm Thick paraffin embedded kidney sections were stained with Mayer's hematoxylin (Merck,109249,) and eosin (Sigma-Aldrich, E6003) (H&E) for qualitative analysis.

Stained H&E sections of both cortex and medulla were scored by an independent pathologist using a scoring system based on previous reports [19, 20]. The scoring system consists of histological lesions in 4 individual renal compartments: Endothelial, Glomerular, Tubular, and Interstitial. The sections were scored on a scale of 0–3 (0 = none; 1 = mild, <25% of the section affected; 2 = moderate, 25–50% of the section affected; 3 = severe, >50% of the section affected).

Coagulation assay

After tissue sampling, the biopsy holes were closed with stitches and kidneys were again perfused at 75 mmHg. Restoring the coagulation cascade was achieved by adding calcium (10mM CaCl2) to the perfusate and pressure and time were recorded during perfusion.

Immunohistochemistry

4-µm thick sections were cut and following rehydration of the tissue samples, antigen retrieval was performed by heating the slides in citrate buffer (pH 6). Primary antibodies against human CD3 (Thermo Scientific, RM-9107-R7), human CD4 (Thermo Scientific, MS-1528-R7), porcine CD31 (Dako, M0823), VCAM-1 (Santa Cruz, SC18854), TLR4 (Santa Cruz, SC13593), CD40 (Invitrogen, PA1-31075), and CCL2 (Santa Cruz, SC 32771), rabbit anti-human C4d (BI-RC4D, Biomedica), and monoclonal anti-C5b-9 (AE11, HM-2167 Hycult) were incubated overnight at 4°C, followed by correspondent fluorescent-labelled secondary antibodies for 1 hour at RT. Nuclei were counterstained using Hoechst 33258 (ThermoFisher). Sections were imaged using SP8-WLL confocal microscopy and displayed using LAS-X software (Leica).

Isolation of pig endothelial cells

After perfusion, tissue from cortex and medulla region of kidney were surgically dissected. The dissected tissue was weighted, placed on a petri dish containing ice-cold digestion HBSS, and cut into small pieces with a scalpel. Samples were then transferred into a 50 mL Falcon tube containing 10 ML digestion buffer (HBSS (cat) supplemented with 0.2% Collagenase Type I (Sigma-Aldrich, Cat#C9891) and 15 mg/mL DNase I and incubated at 37 Celsius degrees in a water bath for 40 min, shaking every 10 min. At the end of incubation, 20 ML ice cold HBSS buffer was added to the digested tissue suspension.

Cell suspension from cortex was filtered with 100 µm cell strainer and then filtered directly in the 40 µm cell strainer. Glomeruli were collected from the 40µm cell strainer with MACS buffer (PBS with 0.5% BSA, 2mM EDTA), centrifuged at 300g for 5 min to collect the pellet, and then digested in 3 ML digestion buffer in 37 Celsius degree water bath for another 20 min, shaking every 10 min. The cell suspension of the flow-through and digested glomeruli were washed twice individually with MACS buffer, pooled together, resuspended in 400ul MACS buffer, and proceed to the MACS purification.

Cell suspension from medulla was filtered with 70 µm cell strain first and then immediately 40 µm cell strain. The flow-through was centrifuged at 300g for 5 min to collect the pellet. The cell pellet was washed twice with MACS buffer and resuspended in 400ul MACS buffer before proceeding with MACS purification.

MACS purification of pig endothelial cells

Isolated cells were pre enriched by MACS after labeling with CD31-biotin (BIO-RAD, MCA1334B,1:300). In briefly, 1.33 µL CD31-Biotin antibody was added to the 400 µL suspended cells. After mixing well, the cells were incubated at 4□ Celsius for 15min. At the end of incubation, the cells were wash twice with MACS buffer and collected by centrifuge at 300g for 5 min. The collected cell pellet was re-suspended in either 320 µL (cortex/glomeruli) or 160 µL (medulla) MACS buffer and either 80 µL (cortex/glomeruli) or 40 µL (medulla) anti-biotin microbeads were added. After incubation at 4 degree for 15 min, the cell pellet was washed with MACS buffer twice and resuspended in 1 ML MACS buffer and enriched with magnetic sorting according to the manufacturer's instruction (LS column from Miltenyi Biotec,130-122-729).

FACS purification of pig endothelial cells

MACS enriched CD31+ cells were labeled with anti-CD31 antibody conjugated with FITC (1:100). Enriched cells were resuspended in 400ul MACS buffer with CD31 antibody for 30 min on ice, protected from light. PI was added before FACS for alive/dead cell gating. The cells were sorted in the 4-way purity mode with FACS Aira II machine (Becton Dickinson) using FACSDiva software.

Single cell library preparation and sequencing

Single cell suspension of freshly isolated cells was resuspended in PBS containing 0.05% BSA and run on a Chromium Single Cell Chip B kit. Single cell RNAseq libraries were prepared using Chromium Single Cell 3' library kit v3 (PN-1000075) and i7 Multiplex kit (PN-120262) according to the manufacturer's protocol. The library quality was determined using a Bioanalyzer 2100. Libraries were sequenced using a deep sequencing MGI sequencer T7, targeting a read depth (50K reads per cells) as suggested by 10x Genomics 3' single-cell RNA kit v3.

Data Processing and in silico EC selection

Fastq files were processed with CellRanger (10x Genomics, version 3.0.2) for alignment to pig reference genome (version Sscrofa 11.1), de-duplication by UMI and expression matrix generation. The gene expression matrix was processed further with Seurat (version 3.2.0) in R (version 3.6.1). Cells were filtered according to the following criteria: (i) genes expressed by less than 3 cells were not considered; (ii) cells that expressed fewer than 300 genes (low quality), and cells that expressed over 3000 genes (potential doublets) were excluded from further analysis; (iii) cells in which over 25% of unique molecular identifiers (UMI) were derived from mitochondrial genome were removed. The data were normalized and log1P transformed using the *NormalizeData* function. For in silico EC selection, (i) contaminated cells which expressed any genes of *PTPRC, CD37, CD53, HBB*, and *CCL21* were filtered; (ii) filtered cells expressed any genes of *PECAM1, CDH5*, and *ICAM2* were processed for further analysis.

Unsupervised EC clustering within group and compartment assignment

For each group independently, filtered ECs isolated from medulla region and cortex region were integrated together with Seurat *IntegrateData* function (dim=1:20). The normalized data were autoscaled and PCA was performed on highly variable genes. To unbiasedly group ECs from glomeruli, cortex and medulla, Unsupervised clustering were performed with Seurat *FindNeighbors* function (dim=1:20) and followed by *FindClusters* function with different resolutions for different groups to generate 3 clusters. Data were visualized by dimension deduction with Seurat *RunUMAP* function (dim=1:20). To annotate clusters with glomeruli ECs, we used canonical marker genes including *PLAT* and *EDH3*. To annotate clusters with medulla and cortex ECs, we combined canonical shared marker *PLVAL* and physical location origin of the ECs.

Correlation analysis of different clusters

For correlation analysis, average expression of the top 2000 highly variable genes in clusters were calculated. Correlation between any two clusters were calculated with *cor* function in stats packages.

Data integration and differential expressed genes identification

Filtered cells from all groups were integrated together with Seurat *IntegrateData* function (dim=1:20). Marker genes in response to human blood perfusion were calculated by comparing with the ECs perfused with pig blood with *wilcoxauc* function in presto package. Genes with high response gene (HRG) (logFC >= 1) and low response gene (LRG) (0.25 < logFC < 1) were subset and used for further analysis.

Unique and common DE gene analysis between WT and KO kidney

Unique and common DE genes with different genotype were analyzed with either *inner_join* or *semi_join* function in *dplyr* package.

Gene ontology and pathway enrichment analysis

For GO over-representation analysis, DE genes were analyzed with *enrichGO* function in *ClusterProfilier* package with GO biological process database (OrgDb=org.Ss.eg.db, pAdjustMethod = "BH").

Immune gene expression analysis

In order to analyze the immune gene set, immune system data were downloaded from NCBI_biosystem (BSID: 1381108 REACTOME: R-SSC-168256). Gene expression matrix containing only the immune gene set was processed to downstream analysis. *FindMarkers* function in Seurat (logFC > 0.25, adjust P < 0.05).

Proteasome score analysis

The expression score of proteasome genes were calculated based on the normalized gene expression data using AddModuleScore function in Seurat. The gene set used for score calculation was downloaded from MSigDB as ".txt" files. Expression of proteasome gene set, which was downloaded from MSigDB

(M7090, Exact source: GO: 0000502). The single cell scores were then subjected to ANOVA test and further paired comparison analysis.

Data visualization

All heatmaps were produced with the *pheatmap* package. Volcano plots of DE genes were produced with *EnhancedVolcano* package. Genes responded in different compartment and genotype were analyzed and visualized with *UpsetR* package.

Data availability

Processed data and raw data produced in this study are available at via the Gene Expression Omnibus (GEO, GSE189512)

Results

An ex-vivo kidney perfusion system for evaluation of xenograft rejection

Before transplanting a xenograft kidney in patients, it is essential to evaluate its safety and efficacy in preclinical human-like conditions. To realize this, we established an ex vivo normothermic pig kidney perfusion system as shown in Fig. 1A. The system was adapted from clinically used systems. We collected kidneys from one wildtype (WT) pig and one genetically modified pig (4KO) lacking three xenoantigens: *GGTA1* encoding the Alpha-1,3-galactosyltransferase, *CMAH* encoding the cytidine monophospho-N-acetylneuraminic acid hydroxylase, and *B4GALNT2* encoding the Beta-1,4-N-Acetyl-Galactosaminyltransferase 2, as well as lacking the swine leukocyte antigen (SLA) class I molecule (SLA-I). The kidneys were perfused with either pig blood (PB) or human blood (HB). Pressure regulated flow supplied the renal artery with carbogen oxygenated whole blood at 37 ˚C (Fig. 1A **and Supplementary Table 1**). Perfusion of the WT kidney with HB resulted in acute rejection and the perfusion could not be sustained longer than for six hours because of clotting activation. Medulla and cortex biopsy samples from WT and 4KO kidneys were histologically examined and analyzed by H&E staining to study signs of rejection.

Extensive renal injury was observed in all renal compartments from WT pig kidneys perfused with HB, while in the 4KO kidney this injury was strongly reduced (Fig. 1B). To quantify the renal injury, H&E images (n=3) from biopsies were scored by an independent and certified pathologist. 14 renal injury parameters were scored using the Endothelial, Glomerular, Tubular, and Interstitial (EGTI) components-based comprehensive histology scoring system[19, 20]. Intratubular hyaline, tubule epithelial cell necrosis and degeneration, interstitium hemorrhage, glomeruli microthrombi and hypercellularity were significant (t-test, p value < 0.005) reduced in the 4KO compared to the WT (Fig. 1C). Particularly, there is less tubular injury in both cortex and medulla in the 4KO than the WT. Broad and strong microthrombosis was observed in the WT glomeruli perfused with HB, which is significantly (t-test, $p < 0.005$) reduced in the 4KO pigs.

Elimination of pig xenoantigens has been shown with benefits on prevention of immune activation in transplantation experiments [3, 21–23]. To validate this in our perfusion model, we stained the perfused kidneys tissues with antibodies against human CD3 and CD4, which are markers of T lymphocytes. We observed strong accumulation of T lymphocytes in the renal cortex of WT pigs perfused with human blood, particularly in the glomeruli, whereas the CD3 or CD4 staining signal in the 4KO kidneys perfused with human blood is strongly reduced (Fig. 1D). CD3 and CD4 is colocalized at the endothelium as validated by co-staining the tissues with endothelial cell marker CD31, indicating that there is an accumulation and infiltration of human T lymphocytes at the endothelium in the WT-HB pig kidney. In addition, we performed complement activation staining on the WT-HB and 4KO-HB tissues. The WT-HB shows C4d and C5b9 positivity mainly within the glomeruli pointing towards activation of the complement system whereas this has disappeared in the 4KO-HB (Fig. 1E). Both coagulation and complement activation have been known as the key cascades in mediated the organ rejection [24, 25]. As a further validation of coagulation, after biopsy sampling, we recalcified the perfused blood re-establishing a physiological coagulation cascade within the perfusion system. Mean arterial pressure was measured in time showing a significant increase in the WT kidney perfused with human blood compared to a moderate increase of the 4KO (Fig. 1F), suggesting that genetic elimination of the SLA-I and three xenoantigens significantly reduces xenograft-rejection associated coagulation. Collectively, we generate an ex vivo system to evaluate xenograft rejection in a preclinical human-like condition and validate that elimination of xenoantigens can significantly reduce the acute renal xenograft rejection-associated kidney injuries.

Single cell RNA sequencing of renal endothelial cells

Blood endothelial cells play important roles in the modulation of xenograft rejection processes. To gain deeper insights into xenograft rejection of renal endothelium and the alteration of molecular signatures of endothelial cells, we isolated renal endothelial cells (REC) from biopsies of perfused kidneys at six hours and analyzed the endothelial cell transcriptome by single cell RNA sequencing. Using a protocol of REC isolation established previously [18], single endothelial cell suspension was obtained by enzymatic digestion, followed by magnetic-activated cell sorting (MACS) and fluorescence-activated cell sorting (FACS)-based enrichment of ECs expressing CD31. In total, we collected RECs from four groups: WT kidney perfused with pig blood (WT-PB), WT kidney perfused with human blood (WT-HB), 4KO kidney perfused with pig blood (4KO-PB) and 4KO kidney perfused with human blood (4KO-HB) (**Supplementary fig. S1**). In each group, single cell RNA sequencing was performed for RECs isolated from cortical and medullary biopsies separately (see methods). To avoid the freeze-thaw caused cell death, sorted cells were immediately subjected to scRNA-seq library construction using the Gel Bead-in-Emulsion (GEM)-based high throughput single cell RNA sequencing technology from 10X genomics, followed by deep sequencing (Fig. 2A). We obtained a sequencing saturation above 70% in all samples, with an average of over 50,000 reads per cells. In total, we captured single cell transcriptome from 93,988 cells. Based on the annotation of pig genome assembly Sscrofa11.1, we detected an average of 1136 transcribed genes per cell and 16,244 expressed genes per samples (**Supplementary Table S2**). Among the 93,988 cells, 2043

cells were removed due to either potential doublets or low quality (see methods). We further performed a marker-based silicon selection to exclude lymphatic cells (*CCL21*[26]), red blood cell (*HBB*), and immune cells (*PTPRC*, CD37(a marker for B cells)[27], and *CD53* (a thymocyte marker)[28]). Only cells expressing endothelial cell markers *PECAM1* (*CD31*, a pan endothelial cell marker), *CDH5* (VE-cadherin, blood vessel marker) [29] and *ICAM2* (intercellular adhesion molecule 2 expressed between endothelial cell junctions) [30] were included for downstream analyses. After all these filtering steps, we obtained high-quality single cell RNA transcriptome from 70,140 RECs (38,519 from WT and 31,611 from 4KO) (**Supplementary Table S3**).

Previous single cell RNA sequencing of RECs in normal mouse kidneys showed that murine RECs exhibit compartmental specific transcriptome [18]. To identify RECs from kidney cortex (cREC), glomeruli (gREC) and medullar (mREC), we applied two approaches to identify RECs from different kidney compartments: (1) Expression of glomeruli markers (*PLAT* and *EDH3*) and cortex/medulla marker *PLVAP*) [31]; (2) Physical biopsy location to separate mRECs and cRECs/gRECs (**Supplementary Figure S1**). Our results showed that pig RECs exhibited distinct compartment specific transcriptome signatures (**Supplementary Figure S1, Supplementary Table S4**), consistent with previous observed of murine RECs [18]. As expected, human blood perfusion strongly affects the REC transcriptome, as seen by both UMAP and correlation analyses (Fig. 2B-D). In WT and 4KO pig kidney, HB-perfused RECs were clustered together and were distinct from the PB-perfused cRECs and gRECs. Unlike cRECs and gRECs, the medullary endothelium (mRECs) displays a similar transcriptomic response to HB and PB. This indicates that HB induces a global transcriptome response ("the endothelial activation response") in the glomerular and cortical endothelium (Fig. 2D). Although histological examination shows clear reduction of kidney injuries and signs of rejections by the elimination of SLA-I and three xenoantigens, single cell RNA sequencing suggests that human blood perfusion still has an effect on the global transcriptome changes in the 4KO pigs. To gain further insights into variation of pathway activities affected by human blood perfusion, we performed Gene Set Variation Analysis (GSVA) for 21 manually curated hallmark gene sets [32]. Figure 2E summarizes endothelial transcriptome changes in a selection of pathways, where in particular changes in the interferon signaling pathways, which is characteristic of T cell mediated rejection, were reduced in the cortical and glomerular endothelial compartment of the 4KO. This was not a reflection of generalized inability to induce an endothelial transcriptomic response upon blood perfusion, as induction of e.g. inflammatory and hypoxia response pathways did not differ between the wild type and 4KO pigs. It should be noted that this analysis only reflects the gene expression variations, but not the activating or inhibitory effect of the corresponding pathways. Our results thus provide the first inventory of pig kidney endothelial cell transcriptome changes caused by human blood perfused at the single cell level and could serve to identify future targets to modulate rejection in pig xenograft transplantation.

Elimination of MHC class I (SLA-I) and three xenoantigens reduces renal endothelial transcriptome alteration caused by human blood perfusion

To further investigate the different response of WT and 4KO RECs to human blood perfusion, we compared cRECs, gRECs, mRECs, respectively, between HB and PB perfused kidneys. Differentially

expressed genes (DEGs) were classified into three classes: High response genes (HRGs, absolute (abs.) log2 fold changes (FC) >= 1, adj. P < 0.05), low response genes (LRGs, 0.25 < abs.log2FC < 1, adj. P < 0.05), and not significantly responding genes (NRG). In WT pigs (Fig. 3A), we identified 1064 up regulated (162 HRGs and 901 LRGs) and 519 down regulated (45 HRGs and 474 LRGs) DEGs in cRECs, 1057 up regulated (167 HRGs and 890 LRGs) and 668 down regulated (60 HRGs and 698 LRGs) DEGs in cRECs, 1055 up regulated (63 HRGs and 992 LRGs) and 406 down regulated (46 HRGs and 360 LRGs) DEGs in mRECs. Although the number of up regulated DEGs is similar between cRECs, gRECs and mRECs in the WT pig, there are more than three-fold less HRGs in the mRECs compared to the cRECs and gRECs. The total number of down regulated DEGs are less (more than 100 genes) in mRECs compared to cRECs and gRECs. The differential gene expression analysis further suggests that HB perfusion triggers higher endothelial transcriptome activation in the cortical regions. Compared to the WT pig, the numbers of DEGs (both HRGs and LRGs) in cRECs, gRECs and mRECs of the 4KO are significantly lower (Fig. 3A, **Supplementary Table S5**). Approximately half of the LRGs in the WT RECs are NRGs in the 4KO RECs. Interestingly, our analysis revealed that approximately half of the HRGs from the WT RECs were LRGs in the 4KO RECs. These findings suggest that elimination of the four genes has substantially (although not completely) reduced HB-triggered endothelium transcriptome activations. To investigate what biological functions these DEGs are mainly involved in, we focus on the HRGs reasoning that the high response genes resembles the strong effects and provide more solid insights into the major effect on endothelial cell transcriptome by the elimination of SLA-I and the three xenoantigens. As shown in Fig. 3B and **fig. S2**, in WT pigs, there were 162, 167 and 63 up-regulated HRGs found in cortex, glomeruli and medulla respectively. In the 4KO pigs, there are less up-regulated HRGs (91, 146 and 4 found in cortex, glomeruli and medulla respectively). There are 65, 95 and 2 commonly up-regulated HRGs in both WT and 4KO kidney in cortex, glomeruli and medulla, respectively. Similarly, there are less down-regulated HRGs found in the 4KO RECs compared to WT RECs (Fig. 3B).

To characterize the genes actively responding to human blood perfusion, we performed gene ontology (GO) analysis for the up-regulated HRGs found in WT only (blue), common (gray), and 4KO only (orange) in all three compartments. Showed in Fig. 3C, the WT only HRGs were enriched in immune related pathways such as regulation of I-κB kinase/NF-κB signaling, toll-like receptor signaling pathway and positive regulation of interleukin-12 production, suggesting that these WT only HRGs are involved in active immune responses. The common HRGs were enriched in functions related to apoptotic process, cell death and would healing. Only the 4KO HRGs were found to be enriched in pathways related to ribosomal assembly and splicing, indicating an effect on the RNA processing machinery. The expression levels for genes commonly involved in these enriched pathways of cortex, glomeruli and medulla RECs were further displayed in the dot plot (Fig. 3D). C–C motif chemokine ligand 2 encoding gene *CCL2* and member of the TNF-receptor superfamily gene *CD40*, which are involved in the regulation of EC apoptosis, inflammatory response, and immune system process, are highly up regulated in the HB-perfused WT RECs but greatly diminished in the 4KO. Genes involved in regulating the NF-kB signaling (i.e. Toll-like receptor 4 encoding gene *TLR4* and TNF-α-induced protein 3-interacting protein 1 encoding gene *TNIP1*), which were more strongly activated in the HB-perfused WT gRECs, were also diminished in the 4KO.

Immunostaining of TLR4, CCL2 and CD40 further confirmed upregulation at the protein level in the HB-perfused WT RECs but not the 4KO RECs (Fig. 3E). Together, our results suggest that human blood perfusion activates the expression of immune regulating genes of WT porcine renal endothelial cells, which was substantially diminished in the 4KO pigs.

Human blood perfusion activates proteasome complex and NF-κB pathway

To further understand the immunoregulatory roles of endothelial cells in xenograft rejection, we generated a subset of immune related genes (717 genes) from the entire dataset. This selected set was subjected to further DE gene analysis (abs.log2FC > 0.25, adjust P < 0.05) and were likewise grouped to WT only DEGs (blue), common DEGs (gray) and 4KO only DEGs (orange). More DEGs genes were up-regulated in all three compartments, indicating that perfusion with human blood led to activation of immune related genes (**Supplementary Table S6**). Within all three compartments, the WT kidney showed the largest group of upregulated unique genes (Fig. 4A). The heatmap in Fig. 4B shows the expression levels of the top selected genes in each group. Within the WT kidney many immune related genes are highly expressed (i.e. *TAP1, ICAM2* and *VCAM1*), while in the KO kidney these genes show a low expression. Our results also showed that there is still a large group of commonly expressed immune genes, indicating a downregulation of the immune response by the 4KO model, but not a complete elimination.

In order to find differences and similarities among different compartments/genotype, we used *upSetR* to visualize the top gene sets which contain either shared or unique genes (Fig. 4C). Interestingly, the largest gene set, which contains 32 genes (see detailed gene list in **supplementary table S6**), was upregulated in all three WT compartments but not the 4KO compartments. GO analysis showed that half of these genes (16/32) belong to the proteasome family, which plays an important role in both the canonical and non-canonical pathways of NF-κB activation [33]. To confirm these findings, we constructed a single cell proteasome score based on the gene expression of proteasome gene set and observed that the proteasome scores in WT glomeruli and cortex were significantly higher than that in the 4KO pigs (figure 4D).

TLR4 and CD40 are essential mediators of NF-κB activation [34, 35], which were upregulated in HB-perfused RECs and significantly reduced in the 4KO RECs (Fig. 3E). To measure if NF-κB regulated genes were also affected, we measured the expression of VCAM by immunostaining and confirmed higher VCAM expression in the HB perfusion WT RECs but less in the 4KO (Fig. 4E). Collectively, our results showed that HB perfusion triggers endothelial activation of genes involved of the NF-κB pathway in WT kidney, while genetic elimination of the porcine MHC class I (SLA-I) and three xenoantigens (GGTA1 CMAH, B4GALNT2) significantly diminishes the activation of these genes (Fig. 4F).

Discussion

The donor endothelium plays a pivotal role in the acute and chronic rejection of the allograft. The binding of preformed antibodies to the xenoantigenic epitopes on porcine endothelial cells triggers the activation

of complement proteins. Activated complement cause further activation and lysis of endothelial cells, leading to the destruction of the graft vasculature and subsequent graft failure. Endothelial cells can also recruit immune cells into the graft, can activate bi-directional signaling with leukocytes and can regulate angiogenesis within the inflammatory reaction[36, 37]. The 4KO porcine model used in this study shows a reduction of the endothelial immune activation response, thus lowering the likelihood of acute vascular rejection upon transplantation. While the genetic deletions in the 4KO model were aimed at reducing cross reactivity with preformed antibodies and hence the acute humoral rejection, our high-resolution analysis of the endothelial transcriptome response shows a much more profoundly suppressed endothelial activation response.

One interesting observation is the reduction in influx of CD4+ human lymphocytes. On top of the well-known three carbohydrate xenoantigenic epitopes that cross react with antibodies, the 4KO also lacks SLA-I. Previous studies have shown that human leukocyte antigen (HLA) antibodies cross-react with the porcine major histocompatibility complex class I, also known as swine leucocyte class I (SLA-I) and hence deletion of SLA-I may further contribute to reducing the risk of humoral rejection [9]. However, the interaction between human T-cell receptors on the lymphocytes in our whole blood perfusion and SLA class I peptide complexes would also be expected to result in T-cell-mediated cytotoxicity against the xenograft vascular endothelium. The lack of SLA-I (and thus inability to present antigens), in combination with the observed absence of upregulation of TAP1 (Transporter associated with antigen processing 1, involved in the transport of degraded peptides before antigen presenting) and lack of co-stimulation with CD40 in the endothelium of the 4KO may also have impeded the cellular effector arm of the acute rejection. This is of particular clinical relevance as in human organ transplantation cellular rejection is the dominant immunological risk and immunosuppressive treatment is primarily targeted towards preventing this.

The profound suppression of the endothelial activation response of the gene-edited endothelial cells is at first sight unexpected. It is, however, of interest that MHC activation has been previously found to result in outside-in signaling and endothelial activation [38, 39]. Specifically, alloantibodies generated by the transplant recipient against MHC-I and MHC-II alloantigens present in the transplanted tissue have been linked to endothelial cell proliferation, survival and migration that can be accompanied by recruitment of inflammatory cells into the transplanted tissue. Phosphorylation of multiple signaling proteins has been observed after antibody-induced MHC-I cross-linking on endothelial cells [40, 41]. One consequence that has been described is the activation of the PI3K-Akt-mTOR pathway that promotes protein synthesis and cell survival. So one hypothesis is that the absence of SLA-I, may have prevented the outside-in signaling through HLA antibodies. In line, PI3K-Akt-mTOR signaling has previously been shown to be a regulator of the NfkB pathway [42, 43].

The use of scRNA seq in our study also allows us to assess endothelial heterogeneity. The kidney cortex, glomeruli and medulla contain unique EC populations (cRECs, gRECs and mRECs, respectively). This diversity in EC populations might arise from exposure to the different microenvironments of these regions

[31]. Our data show that the porcine cRECs, gRECs and mRECs exhibit compartment-specific transcriptome profile, similar to the finding in murine kidneys [18]. In response to human blood perfusion the endothelial activation response is more pronounced in the cortical and in particular glomerular endothelium and, vice versa, the absence of the endothelial activation response in the 4KO is most pronounced in these compartments. In fact, there was little difference in the transcriptome response between HB and PB in the medullary compartment. This is in line with our previous observation that the medullary endothelium has a specific phenotype that is adapted to the hypoxic hyperosmolar milieu while the cortical endothelial cells are the ones that express MHC class II and response signalling pathways to mediate interaction with blood components [31].

Our study also has some limitations. In this study, the use of blood is from a single donor, which therefore does not take into account person-to person variability in preformed antibodies. Due to the limited availability of the 4KO animal, only one pig could be recruited into this study. Although this has provided very importantly insights into the protection of kidney injury and rejection by the genetic modifications, future studies should be carried out using more animals. A third limitation is that this study only looks at the acute immune rejection processes and lack of insights into the longer-term outcome. It has recently been shown screening and removal of anti-pig antibodies and complete CD4+ T-cell depletion of the recipient led to long-term survival of pig-to-rhesus macaque renal xenografts [44]. While not clinically applicable, this points towards the feasibility for longer term survival of xenografts when the immunological barrier is overcome.

Very recently a GGTA1 KO kidney xenograft was transplanted in human brain dead recipient that was kept on a ventilator for a 54 hour follow up without rejection, rekindling the interest to use xenografts as an alternative solution to transplant organ shortage. Clearly many hurdles still need to be overcome to allow for clinical translation including the (long term) safety, function and ethical aspects. However, also the current study provides a further translational perspective that advanced genetic editing of pigs may generate xenografts that can accommodate to human blood in an ex vivo perfusion. In addition, our study provides in-depth insight in the endothelial activation pathways during xenograft rejection and how these are being modified in the 4KO while the accessible repository of transcriptome changes may lead to the discovery of new targets for anti-rejection therapy.

Declarations

Acknowledgments

We thank Prof Dietmar Zehn and Kristiyan Kanev, TU Munich FACS core facility, for help with sorting of endothelial cells**.** We thank Trine Skov Petersen, department of biomedicine, for her technical help and assistance. The study is partially supported by the Independent Research Fund Denmark – Sapere Aude Starting Grant (8048-00072A to L.L.), the Novo Nordisk Foundation (NNF21OC0071718 to L.L.), the German Research Foundation (DFG, to A.S.), and Transregio Collaborative Research Center 127 (to A.S.).

Author Contributions: Conceptualization**,** L.L., A.S., T.J.R., and Y.L.; Methodology, L.L., F.M.R.W., K.F., and M.A.E; Investigation, L.L., F.M.R.W., K.F., M.A.E, A.M.A.G, B.R., A.F., Y.W., M.R.H., A.M., F.W., X.L., X.X., L.X., P.L., F.C., H.J., R.R., K.S., C.K., A.S., T.J.R., and Y.L.; Writing – Original Draft, L.L., F.M.R.W, T.J.R., and Y.L.; Writing -review and editing, all authors; Funding acquisition, L.L., A.S., T.J.R, and Y.L.; Resources: H.Y., L.B., R.R., K.S., C.V.K., A.S., T.J.R., and Y.L.; Supervision, H.Y., L.B., R.R., K.S., C.V.K., A.S., T.J.R., and Y.L.

Competing Interest Statement: Authors declare no competing interest.

References

1. Augustine, J. Kidney transplant: New opportunities and challenges. *Cleve Clin J Med* **85**, 138–144 (2018).
2. Cooper, D.K. et al. The pathobiology of pig-to-primate xenotransplantation: a historical review. *Xenotransplantation* **23**, 83–105 (2016).
3. Ma, D. et al. Kidney transplantation from triple-knockout pigs expressing multiple human proteins in cynomolgus macaques. *Am J Transplant* (2021).
4. Lai, L. et al. Production of alpha-1,3-galactosyltransferase knockout pigs by nuclear transfer cloning. *Science* **295**, 1089–1092 (2002).
5. Niu, D. et al. Inactivation of porcine endogenous retrovirus in pigs using CRISPR-Cas9. *Science* **357**, 1303–1307 (2017).
6. Yang, L. et al. Genome-wide inactivation of porcine endogenous retroviruses (PERVs). *Science* **350**, 1101–1104 (2015).
7. Cowan, P.J., Cooper, D.K. & d'Apice, A.J. Kidney xenotransplantation. *Kidney Int* **85**, 265–275 (2014).
8. Cooper, D.K.C. et al. Clinical Pig Kidney Xenotransplantation: How Close Are We? *J Am Soc Nephrol* **31**, 12–21 (2020).
9. Fischer, K. et al. Viable pigs after simultaneous inactivation of porcine MHC class I and three xenoreactive antigen genes GGTA1, CMAH and B4GALNT2. *Xenotransplantation* **27**, e12560 (2020).
10. Langin, M. et al. Cold non-ischemic heart preservation with continuous perfusion prevents early graft failure in orthotopic pig-to-baboon xenotransplantation. *Xenotransplantation* **28**, e12636 (2021).
11. Zhu, A. & Hurst, R. Anti-N-glycolylneuraminic acid antibodies identified in healthy human serum. *Xenotransplantation* **9**, 376–381 (2002).
12. Byrne, G.W., Du, Z., Stalboerger, P., Kogelberg, H. & McGregor, C.G. Cloning and expression of porcine beta1,4 N-acetylgalactosaminyl transferase encoding a new xenoreactive antigen. *Xenotransplantation* **21**, 543–554 (2014).
13. Yue, Y. et al. Extensive germline genome engineering in pigs. *Nat Biomed Eng* **5**, 134–143 (2021).
14. Adams, A.B. et al. Xenoantigen Deletion and Chemical Immunosuppression Can Prolong Renal Xenograft Survival. *Ann Surg* **268**, 564–573 (2018).

15. Weissenbacher, A., Vrakas, G., Nasralla, D. & Ceresa, C.D.L. The future of organ perfusion and re-conditioning. *Transpl Int* **32**, 586–597 (2019).
16. Elliott, T.R., Nicholson, M.L. & Hosgood, S.A. Normothermic kidney perfusion: An overview of protocols and strategies. *Am J Transplant* **21**, 1382–1390 (2021).
17. Langin, M. et al. Consistent success in life-supporting porcine cardiac xenotransplantation. *Nature* **564**, 430–433 (2018).
18. Dumas, S.J. et al. Single-Cell RNA Sequencing Reveals Renal Endothelium Heterogeneity and Metabolic Adaptation to Water Deprivation. *J Am Soc Nephrol* **31**, 118–138 (2020).
19. Khalid, U. et al. Kidney ischaemia reperfusion injury in the rat: the EGTI scoring system as a valid and reliable tool for histological assessment. *Journal of Histology & Histopathology* **3**, 1–7 (2016).
20. Pool, M.B.F., Hartveld, L., Leuvenink, H.G.D. & Moers, C. Normothermic machine perfusion of ischaemically damaged porcine kidneys with autologous, allogeneic porcine and human red blood cells. *PLoS One* **15**, e0229566 (2020).
21. Cascalho, M. & Platt, J.L. The immunological barrier to xenotransplantation. *Immunity* **14**, 437–446 (2001).
22. Cui, Y. et al. Evidence for GTKO/beta4GalNT2KO Pigs as the Preferred Organ-source for Old World Nonhuman Primates as a Preclinical Model of Xenotransplantation. *Transplant Direct* **6**, e590 (2020).
23. Shim, J. et al. Human immune reactivity of GGTA1/CMAH/A3GALT2 triple knockout Yucatan miniature pigs. *Transgenic Res* (2021).
24. Amara, U. et al. Interaction between the coagulation and complement system. *Adv Exp Med Biol* **632**, 71–79 (2008).
25. Gavriilaki, E. et al. Linking Complement Activation, Coagulation, and Neutrophils in Transplant-Associated Thrombotic Microangiopathy. *Thromb Haemost* **119**, 1433–1440 (2019).
26. Manzo, A. et al. CCL21 expression pattern of human secondary lymphoid organ stroma is conserved in inflammatory lesions with lymphoid neogenesis. *Am J Pathol* **171**, 1549–1562 (2007).
27. Barrena, S. et al. Aberrant expression of tetraspanin molecules in B-cell chronic lymphoproliferative disorders and its correlation with normal B-cell maturation. *Leukemia* **19**, 1376–1383 (2005).
28. Puls, K.L., Hogquist, K.A., Reilly, N. & Wright, M.D. CD53, a thymocyte selection marker whose induction requires a lower affinity TCR-MHC interaction than CD69, but is up-regulated with slower kinetics. *Int Immunol* **14**, 249–258 (2002).
29. Gory-Faure, S. et al. Role of vascular endothelial-cadherin in vascular morphogenesis. *Development* **126**, 2093–2102 (1999).
30. Huang, M.T. et al. Endothelial intercellular adhesion molecule (ICAM)-2 regulates angiogenesis. *Blood* **106**, 1636–1643 (2005).
31. Dumas, S.J. et al. Phenotypic diversity and metabolic specialization of renal endothelial cells. *Nat Rev Nephrol* **17**, 441–464 (2021).

32. Hanzelmann, S., Castelo, R. & Guinney, J. GSVA: gene set variation analysis for microarray and RNA-seq data. *BMC Bioinformatics* **14**, 7 (2013).
33. Chen, Z.J. Ubiquitin signalling in the NF-kappaB pathway. *Nat Cell Biol* **7**, 758–765 (2005).
34. Karki, R. & Igwe, O.J. Toll-like receptor 4-mediated nuclear factor kappa B activation is essential for sensing exogenous oxidants to propagate and maintain oxidative/nitrosative cellular stress. *PLoS One* **8**, e73840 (2013).
35. Hostager, B.S. & Bishop, G.A. CD40-Mediated Activation of the NF-kappaB2 Pathway. *Front Immunol* **4**, 376 (2013).
36. Piotti, G., Palmisano, A., Maggiore, U. & Buzio, C. Vascular endothelium as a target of immune response in renal transplant rejection. *Front Immunol* **5**, 505 (2014).
37. Cardinal, H., Dieude, M. & Hebert, M.J. Endothelial Dysfunction in Kidney Transplantation. *Front Immunol* **9**, 1130 (2018).
38. Salehi, S. et al. Outside-in HLA class I signaling regulates ICAM-1 clustering and endothelial cell-monocyte interactions via mTOR in transplant antibody-mediated rejection. *Am J Transplant* **18**, 1096–1109 (2018).
39. Muntjewerff, E.M., Meesters, L.D., van den Bogaart, G. & Revelo, N.H. Reverse Signaling by MHC-I Molecules in Immune and Non-Immune Cell Types. *Front Immunol* **11**, 605958 (2020).
40. Jin, Y.P. et al. RNA interference elucidates the role of focal adhesion kinase in HLA class I-mediated focal adhesion complex formation and proliferation in human endothelial cells. *J Immunol* **178**, 7911–7922 (2007).
41. Jindra, P.T., Jin, Y.P., Rozengurt, E. & Reed, E.F. HLA class I antibody-mediated endothelial cell proliferation via the mTOR pathway. *J Immunol* **180**, 2357–2366 (2008).
42. Dan, H.C. et al. Akt-dependent regulation of NF-{kappa}B is controlled by mTOR and Raptor in association with IKK. *Genes Dev* **22**, 1490–1500 (2008).
43. Hassan, B., Akcakanat, A., Holder, A.M. & Meric-Bernstam, F. Targeting the PI3-kinase/Akt/mTOR signaling pathway. *Surg Oncol Clin N Am* **22**, 641–664 (2013).
44. Kim, S.C. et al. Long-term survival of pig-to-rhesus macaque renal xenografts is dependent on CD4 T cell depletion. *Am J Transplant* **19**, 2174–2185 (2019).

Figures

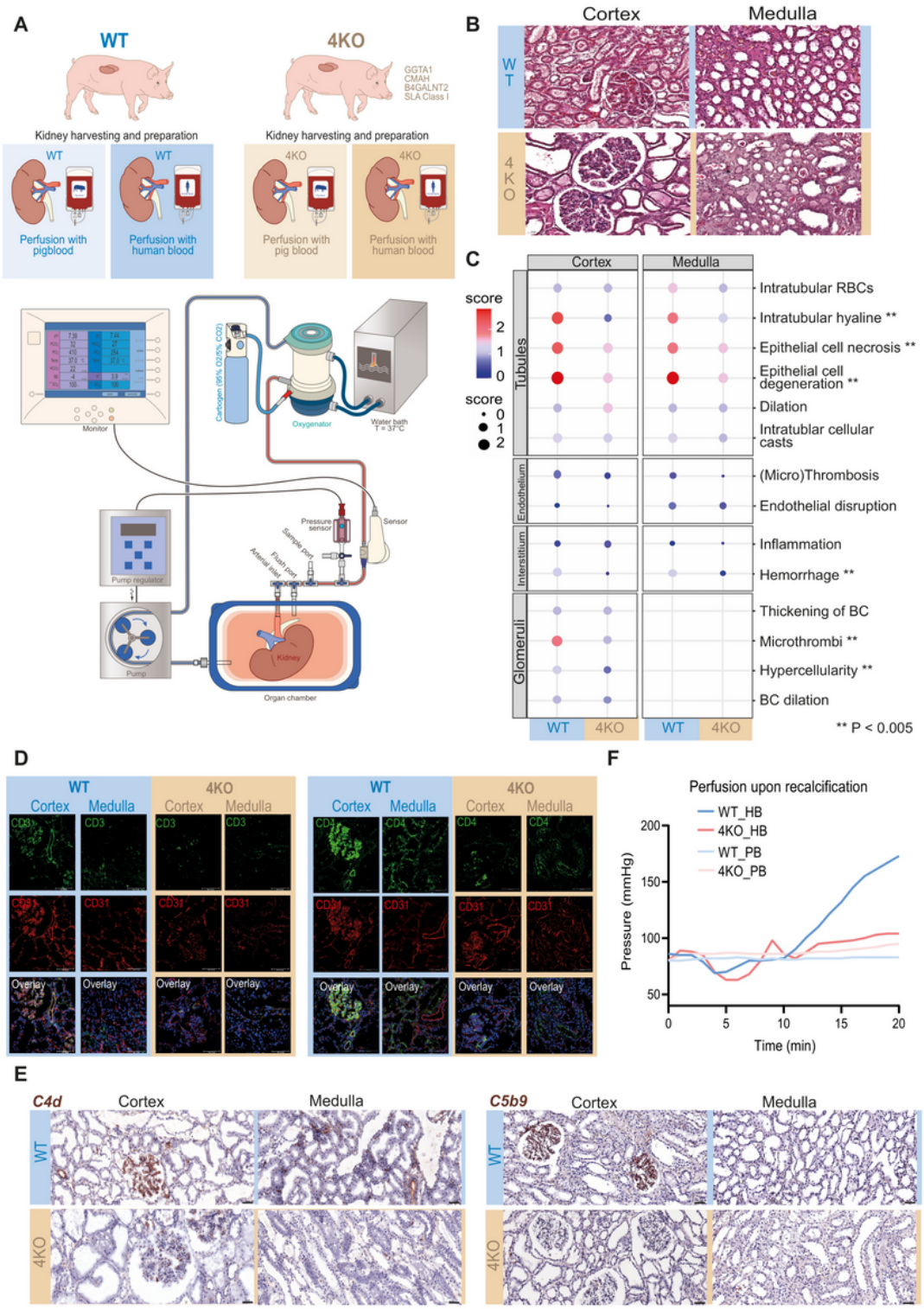

Figure 1

Characterization of pig kidney injury and immune rejection using an ex vivo blood perfusion system.

A, Ex vivo pig kidney perfusion system enabling normothermic oxygenated machine perfusion of four kidneys simultaneously. B, H&E stained sections of cortex and medulla of both WT and KO kidney perfused with human blood for 6 hours. Scalebar 50 μm. C, Dot plot quantification of the pathological

injury scored per region for both WT and KO showing extensive damage in the WT kidney which is less in the KO. Dot size and dot color display the same information. D, Immunofluorescence staining of human CD3 and CD4 combined with a porcine specific CD31 antibody of WT and 4KO kidney sections showing a lower T-cell infiltration in the 4KO. Scalebar 100 μm. E, Immunohistochemical staining of human C4d and C5b9 showing complement activation in the glomeruli of the WT whereas this is absent in the 4KO. Scalebar 50 μm. F. Measurement of pressure in time after recalcification of the blood perfusate re-establishing a physiological coagulation cascade within the perfusion system (performed after tissue biopsy sampling).

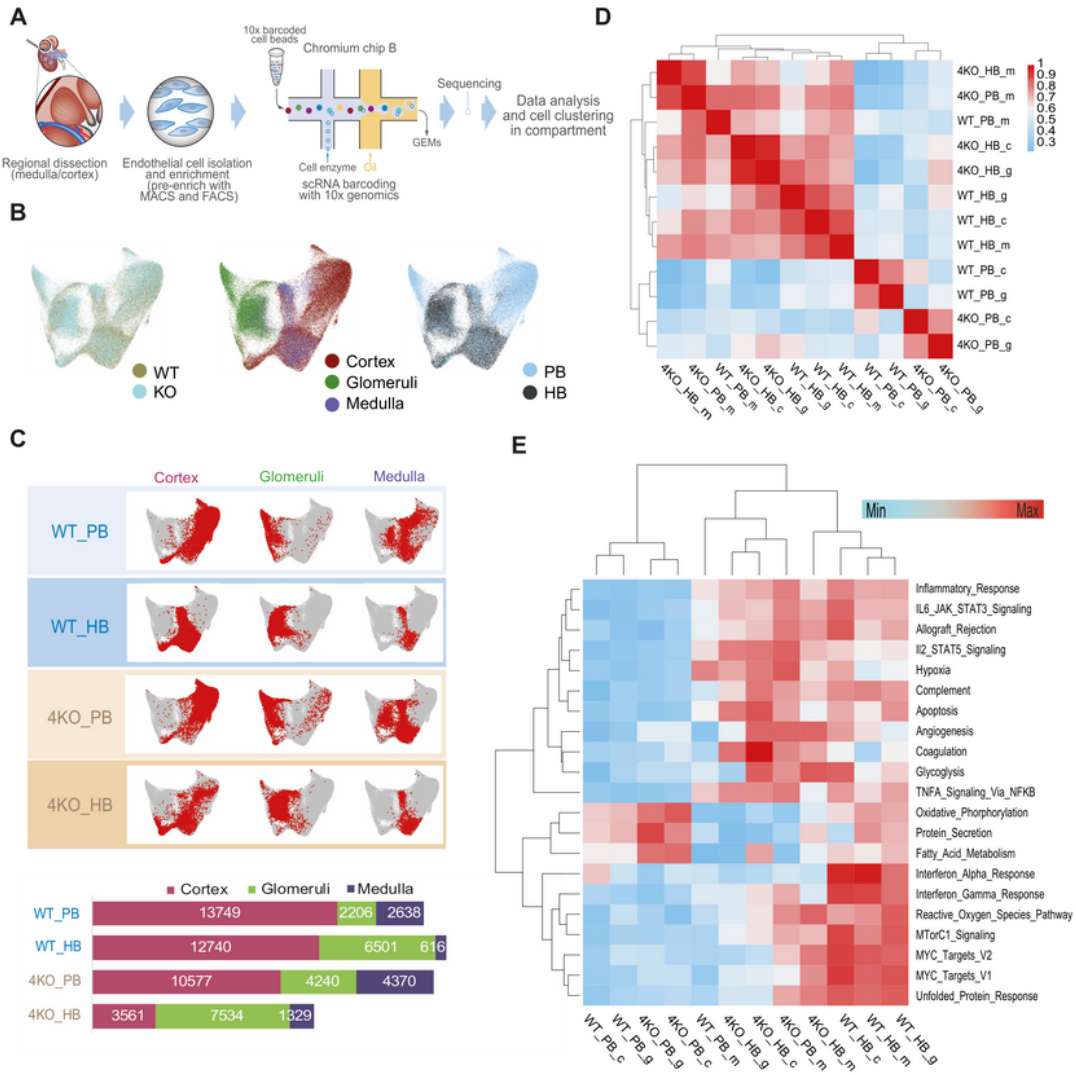

Figure 2

Single cell RNA sequencing of kidney endothelial cells

A, Schematic illustration of the work flow of tissue processing, renal endothelial cell isolation, single cell RNA sequencing, and analysis. MACS, Magnetic-activated cell sorting; FACS, Fluorescence-activated cell sorting. B, UMAP visualization of endothelial cells based on genotypes (left), renal compartments

(middle), or perfusion blood types (right). C, UMAP visualization and highlight of endothelial cells from a specific renal compartment of WT or 4KO pig kidney perfused with human blood (HB) or pig blood (PB), distribution of cortex, medulla and glomeruli cells within each kidney. Cell numbers of each compartment were displayed in bar graph. D, Heatmap plot of correlations between the 12 groups of ECs based on the top 2000 highly variable genes. E. Heatmap showing the gene set enrichment analysis of 21 hallmark gene sets in the 12 groups of ECs.

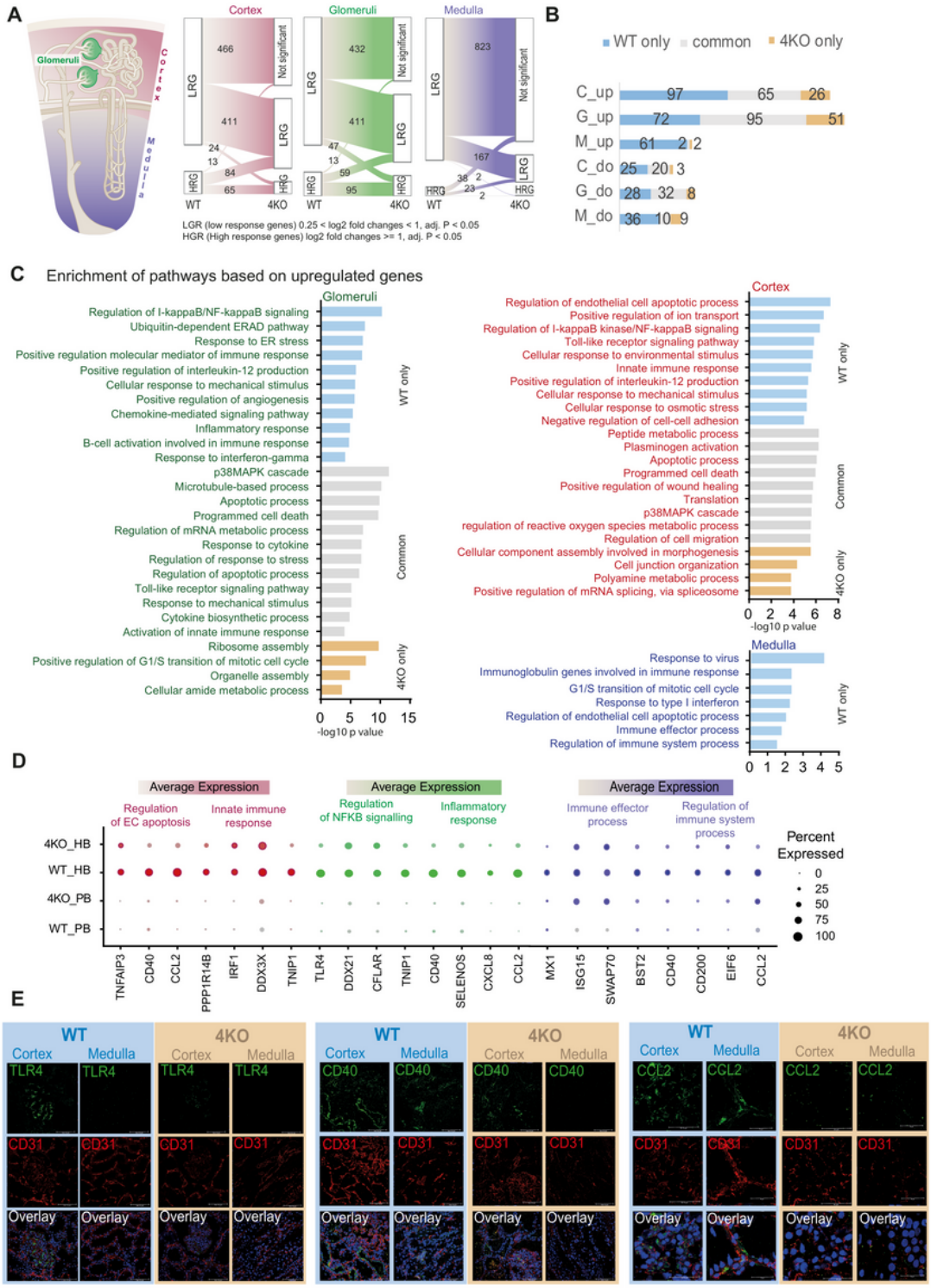

Figure 3

Effects of human blood perfusion on EC gene expression and functions. A, Identification differentially expression genes.

RECs were divided into three groups: cRECs (red), gRECs (green) and mRECs (violet). In each group the differentially expressed (DE) genes were classified into three classes: high response genes (HRG), low

response genes (LRG) and non-significantly response genes. The right side of the figure shows how the DE genes in each class in the WT relate to 4KO illustrating reduced transcriptome alterations in the 4KO. B, Table showing the numbers of significant up-and down regulated HRGs for each compartment in WT only (blue), 4KO only (orange), and both WT and 4KO (common, gray). C, Enrichment of pathways based on upregulated LRGs for each group (WT only, 4KO only and common) and each compartment (cortex, glomeruli, medulla). D, Dot plot of the gene expression levels within the most relevant pathways showing a reduced expression of inflammatory and injury related genes within the 4KO compared to WT. E, Immunofluorescence staining TLR4, CD40 and CCL2 in WT and 4KO pig kidney perfused with human blood. Scalebar 100 μm.

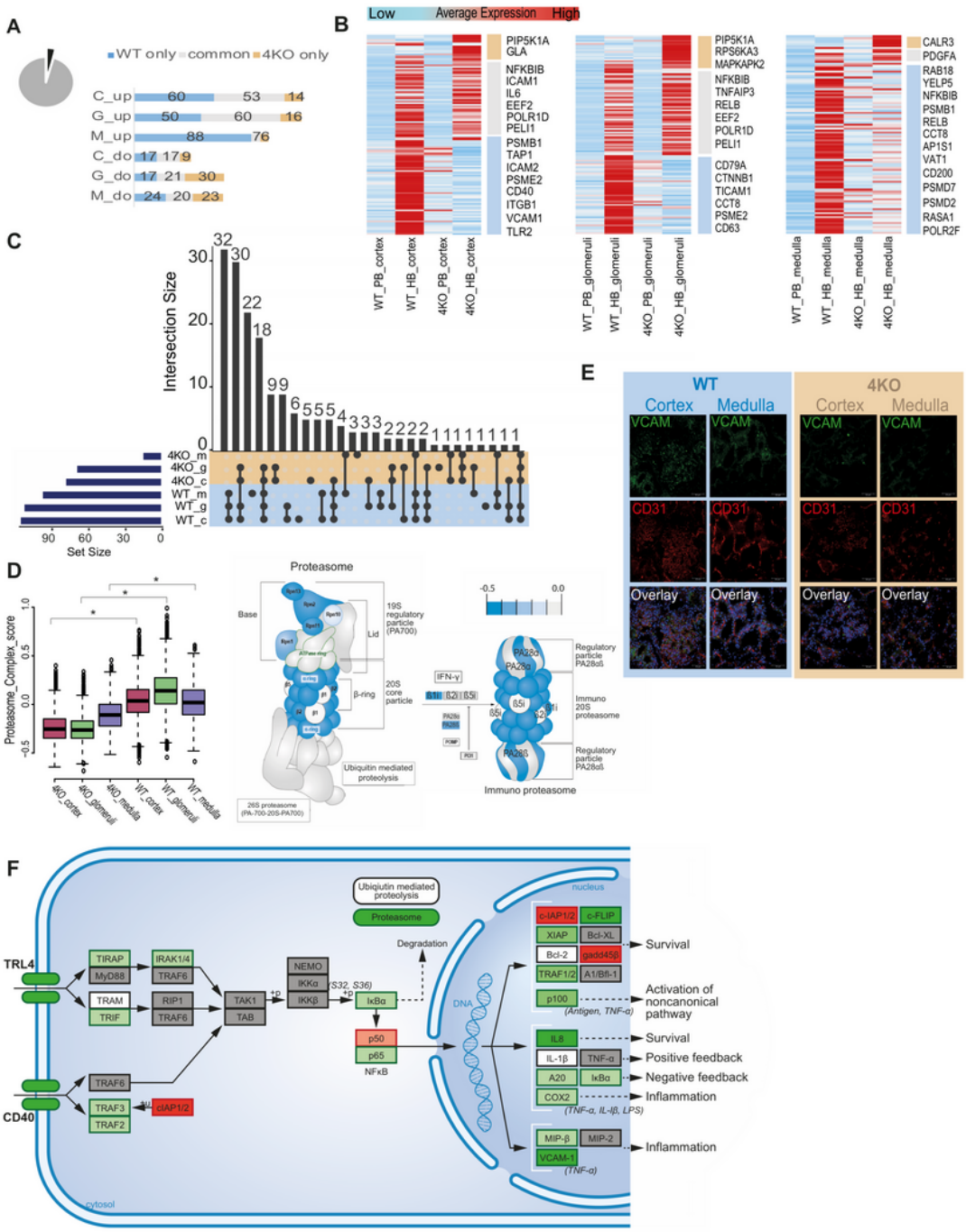

Figure 4

Effect of human blood perfusion on the expression of immune regulatory genes in RECs.

A, Numbers of significantly up-and down regulated genes (log2 fold change more than 0.25, and adjusted p value less than 0.05) for each compartment in WT only (blue), 4KO only (orange) and commonly (gray) expressed within the 717 immune regulatory genes. B, Heatmap showing the expression level of immune

related genes within each compartment for each condition. At least half of the genes which are high expressed in the WT kidney after perfusion with human blood are low expressed in the 4KO kidney, showing a clear reduction in the activation of immune regulatory genes. C, upSetR analysis to visualize the top gene sets which contain either shared or unique genes. The top gene set contains 32 genes and is solely expressed by the WT in all three compartments. D, Proteasome score for each compartment in WT and 4KO kidney calculated based on the RNA expression levels showing a lower significant proteasome score in the 4KO in all three compartments. *, p value<0,00001. The right side shows a visualization of the proteasome complex including its expression within the 4KO (all compartments combined). The expression of the immunomodulating part of the proteasome complex (iB1) is lower in the 4KO. E, Immunofluorescence staining of VCAM in WT and 4KO pig kidney perfused with human blood, showing a lower expression within the 4KO in both cortex and medulla. Scalebar 50 µm. F, Visualization of the NF-kB pathway including TRL4 and CD40 (stainings in figure 3), proteasome complex, IL-8 and VCAM. Genes expression levels of the 4KO kidney (all compartments combined) are displayed within the pathway figure.

Supplementary Files

This is a list of supplementary files associated with this preprint. Click to download.

- TableS5compartmentDEGs.xlsx
- TableS4compartmentmarkergenesforeachgrouptop50.xlsx
- TableS6immuneDEGs.xlsx
- TableS3cellnumbersbeforeandafterinsiliconselection.xlsx
- FigureS1.png
- TableS1Perfusionparameters.xlsx
- FigureS2venn.png
- TableS2sequencinginformationandanalysisparameters.xlsx
- NCXenoXSI041221.docx